Int. J. Electrochem. Sci., 8 **(2013)** 2468 - 2478

International Journal of
ELECTROCHEMICAL
SCIENCE
www.electrochemsci.org

Chemical Deposition and Electrocatalytic Activity of Platinum Nanoparticles Supported on TiO_2 Nanotubes

M.N. Shaddad[1,*], *A.M. Al-Mayouf*[1, a], *M.A. Ghanem*[1,3,*], *M.S. AlHoshan*[2, a], *J.P. Singh*[1], *A.A Al-Suhybani*[1]

[1]Chemistry Department, College of Science, King Saud University, Riyadh 11451, Saudi Arabia
[2]Chemical Engineering Department, College of Engineering, King Saud University, Riyadh 11421, Saudi Arabia
[3]Permanent address: Science & Math. Department, Faculty of Petroleum & Mining Engineering, Suez Canal University, Suez Egypt
[a]The Hydrogen Energy Research Group, Sustainable Energy Technologies (SET), King Saud University, Riyadh, Saudi Arabia
[*] E-mail: maghanem25@yahoo.com; mshadad@ksu.edu.sa

Received: 25 November 2012 / *Accepted:* 27 December 2012 / *Published:* 1 February 2013

Platinum electrocatalysts (Pt-B/TON-N_2, Pt-B/TON-air and Pt-H/TON-air) incorporated on annealed titanium oxide nanotubes (TONs) have been successfully synthesized by chemical deposition method using sodium borohydride and hydrazine, reducing agents. TONs were firstly prepared by anodization of pure Ti foil in HF solution followed by annealing in air and N_2 atmosphere. The morphology and structure of the electrocatalysts were characterized by scanning (SEM), transmission (TEM) electron microscopies, X-ray diffraction (XRD), energy dispersive X-ray spectroscopy (EDS) and electrochemical techniques. SEM, TEM, XRD and EDX characterization indicate the presence of platinum nanoparticles with diameter less than 50 nm and uniformly incorporated into TON arrays. The electrocatalytic activities results show that the Pt-B/TON-N_2 catalyst has higher catalytic activity for the oxygen reduction reaction (ORR) and hydrogen evolution reaction (HER) compared with Pt-B/TON-air and electrodes prepared using hydrazine as reducing agent because the better conductivity. In addition, the Pt-B/TON-N_2 catalyst exhibits better poison tolerance and two times higher methanol oxidation current density than that reported for Pt/carbon catalyst. This suggests that the Pt-B/TON-N_2 catalyst supported on TON-N_2 has promising potential applications in electrocatalyst reactions.

Keywords: titanium oxide, nanotubes, Pt nanoparticles, electrocatalysis, reducing agent, electroless.

1. INTRODUCTION

Increasing energy demands, depletion of fossil fuel reserves and environmental pollution have motivated the search for other energy conversion devices with high efficiency and low emissions. The

widespread of fuel cells and subsequent attempts to make the technology economically competitive make more attention to be focused on lowering the cost of the membrane electrode assembly (MEA) and, specifically the catalysts used for the oxygen reduction reaction (ORR). Fuel cells fueled by hydrogen and oxygen; or small organic molecules such as methanol may have the ability to meet these demands [1]. Direct methanol fuel cells (DMFCs) have been considered as the ideal clean fuel cell system for portable electronic devices and transportation applications, as they are superior to other kinds of fuel cells in weight–volume energy densities and working conditions, etc [2]. In an acidic medium, the most efficient catalysts for DMFC is platinum (Pt) based catalysts. The electrocatalytic activity of catalysts for methanol electro-oxidation is dependent on many factors [3] . Of these, is the catalyst support and its surface condition are essential for the catalyst to increase its electrocatalytic activity [4]. In previous studies, a variety of carbon supports have been investigated based on their high chemical stability and good electron conductivity, etc [5].

The catalytic properties of the platinum catalyst depend on the properties of support [7] such as its surface area and electronic properties which are considered important to produce high catalytic activity [8]. One-dimensional catalyst supports, such as titanium oxide nanowires [9], nanoribbons [10], nanotubes and nanorods [11, 12], have attracted considerable attention recently. Titanium oxide nanotubes (TONs) are of particular significance due to their superior physicochemical properties and potential applications in electrocatalysis [13], photocatalysis [14], and energy use including hydrogen storage [15] and lithium batteries [16]. TON arrays have attracted much attention as catalyst support because of their large specific surface area, favorable surface chemistry, good biocompatibility, and allow efficient access for the catalyst materials [17]. For example, the surface chemistry of TONs can be easily modified through coordination with amine and carboxyl groups, and used in detection of electroactive molecules or as biosensors [18, 19]. There are three general approaches for synthesis the titanium oxide nanotubular structures, namely, template-assisted fabrication [20], alkaline hydrothermal synthesis [21], and anodic oxidation or anodization of titanium foil [22]. The advantage of TONs produced by anodization is that they are readily attached onto a titanium substrate and form oriented, aligned perpendicular to the substrate, which offers much improved electron transfer pathways and catalyst accessibility than non-oriented (random mixtures) structure. As a result, this oriented TON has a great potential as electrochemical electrodes for highly sensitive biosensor applications. However, an obstacle preventing TON arrays from wide spread applications is their irreversible electrode reactions. Reduction peaks were commonly observed, but no oxidation peaks can be seen in the reverse potential scan during the cyclic voltammetric measurements due to the low electrical conductivity of titanium oxide [23, 24]. Annealing in different gases is considered to be one possible approach to narrow the band gap and enhance the electrical conductivity [25, 26].

Chemical deposition is among the most straightforward and efficient methods used to fabricate Pt-based nanomaterials [27] with the help of a chemical reducing agent. A variety of reducing agents have been employed to synthesize Pt nanoparticles (NPs) [30, 31]. The most commonly used reducing agents are ethylene glycol [32] and sodium borohydride [33]. Metz et al. [34] synthesized Pt NPs on vertically aligned carbon nanofibers (VACNFs) and Knupp et al. [35] also fabricated Pt nanotubules on aluminum sheets using hydrazine as a reducing agent. Herricks et al. [36] synthesized Pt NPs on carbon nanotubes and carbon nano-fibers using a polyol synthesis method with ethylene glycol as the

reducing agent. Guo et al. [37] used sodium borohydride as a reducing agent and citric acid (CA) as a stabilizing agent to prepare Pt NPs. Wells et al. [38] employed a polyol process with sodium nitrate to control the morphology of the synthesized Pt NPs, where ethylene glycol served as both the reducing agent and solvent.

Recently we developed TONs substrate with improved conductivity by annealing at different temperatures under air atmosphere [39]. In this work we demonstrate the chemical deposition and characterization of Pt NPs (Pt-B/TON-N_2, Pt-B/TON-air and Pt-H/TON-air) loaded on highly conducted TONs support using hydrazine and sodium borohydride as reducing agents. TONs support was pre-annealed in air and N_2 atmosphere at 450 ^{0}C which highly improve the electrical conductivity. Also the electrocatalytic activity of the prepared Pt/TONs catalysts was evaluated for the oxygen reduction reaction (ORR), hydrogen evolution reaction (HER) and methanol electro-oxidation reaction (MOR) in acidic and alkaline media.

2. EXPERIMENTAL

Ti foil (purity > 99.5% thickness 0.25 mm), dihydrogen hexachloroplatinate (IV) hydrate ($H_2PtCl_6.6H_2O$ > 99.99%) and $PdCl_2$ (purity > 99.99%) were purchase from Alfa Aesar. HF (purity 39-43%) from QualiKems, $NaBH_4$ (purity > 98.0%, WINLAB), NH_2NH_2 (> 99.0%) and $C_2H_4(NH_2)_2$ (> 99.0%) were obtained from PS. H_2SO_4 (> 98.0%, BDH, AR), CH_3OH (purity > 99.5%, AVONCHEA, AR), NaOH solution 32% in water (Fluka), $SnCl_2.2H_2O$ (Sigma Aldrich, ACS reagent) and HNO_3 (purity >99.0% , BDH, AR). All aqueous solutions were prepared with deionized water produced by Milli-Q (resistance 18.2 MΩ cm, Millipore, Inc.).

Highly ordered TONs substrate were fabricated by electrochemical anodic oxidation of Ti foil according to a method reported in the literature [40]. Ti foils with an area of 20 ×30 mm and thickness of 0.25 mm were used as starting material in order to obtain the TON arrays. All Ti sheets were washed in deionized water and degreased in an ultrasonic bath in isopropanol, acetone and finally washed with DI water followed by air-drying. The anodization was performed at room temperature using two-electrode electrochemical cell with the Ti foil as the anode and a Pt foil as the cathode and the distant between them was maintained at 2 cm. The substrates were prepared by applying anodizing voltage of 20 V using DC power supply (E3612A, Agilent Technologies) in 0.5 wt% HF solution for 20 min. After anodization, samples were washed with deionized water and the as-anodized TONs were subsequently annealed at 450 °C in air or N_2 atmosphere (designated as TON-air and TON-N_2 respectively) for 3 h with heating and cooling rate of 5 °C min^{-1} to induce anatase crystallization.

Before Pt chemical deposition, TON substrates were firstly sensitized for 30 min in 0.3% (wt) $SnCl_2$ + 3% (wt) HCl followed by activation in 0.1% (wt) $PdCl_2$+ 2.0% (wt) HCl solutions respectively. After sensitization and activation of TON arrays, Pt was deposited on TON-air and TON-N_2 by immersing in 25 ml solution containing 0.1 g $H_2PtCl_6.4H_2O$, 0.1 ml ethylenediamine ($C_2H_4(NH_2)_2$) and 0.1 g NH_2NH_2 or 0.1 g $NaBH_4$. The electroless deposition process was performed at 63 ^{0}C for 30 min with pH controlled at 13 by adding NaOH solution.

The TON substrates and deposited Pt catalysts were characterized by XRD (Ultima IV, X-ray diffractometer: Rigaku) with Cu-K_α radiation (λ = 0.15418 nm; 40 kV and 40 mA). The morphology of the samples was examined using a high-performance, scanning electron microscope (SEM; JSM-6380LA) fitted with energy dispersive X-ray spectroscopy (EDS) (Vantage 4105, NORAN) and transmission electron microscope (TEM; JEM-1400). The metal loading of Pt deposited on the TON supports was determined by inductively coupled plasma atomic emission spectrometry (ICP-AES).

The cyclic voltammetry (CV) was performed in a conventional three-electrode single-compartment Pyrex glass cell using a computerized potentiostat/galvanostat (Autolab, PGSTAT30) with NOVA 1.8 software. The reference and the auxiliary electrodes were SCE and pure Pt-foil, respectively. The current was divided by 0.68 cm^2 the geometric area of working electrode.

3. RESULTS AND DISCUSSION

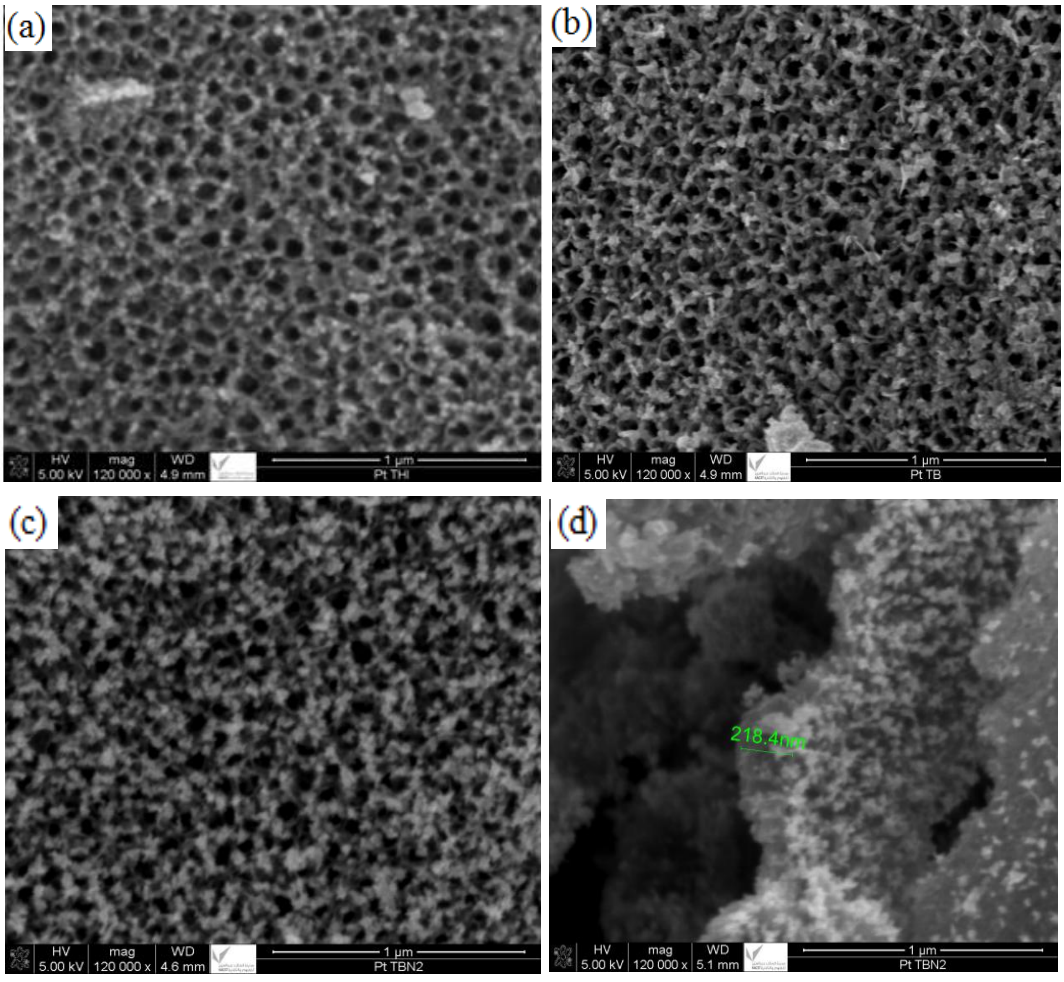

Figure 1. SEM images for Pt catalysts supported on TONs, (a) Pt-H/TON-air, (b) Pt-B/TON-air, (c) Pt-B/TON-N_2 and (d) cross-sectional view for Pt-B/TON-N_2 electrodes.

Figs. 1 shows the surface morphology of Pt nanoparticles deposited on TONs support annealed in air and N_2 at 450 °C for 3 h and using reducing agent of (a) hydrazine (Pt-H/TON-air), (b) $NaBH_4$ (Pt-B/TON-air), (c) $NaBH_4$ (Pt-B/TON-N_2) and (d) shows the cross-sectional for Pt-B/TON-N_2. Homogenously dispersed Pt nanoparticles clearly can be seen on the TON-air and TON-N_2; with some particles located at the rims and inside of highly packed TONs. From the cross section image we can estimate the TONs thickness at about 250 nm.

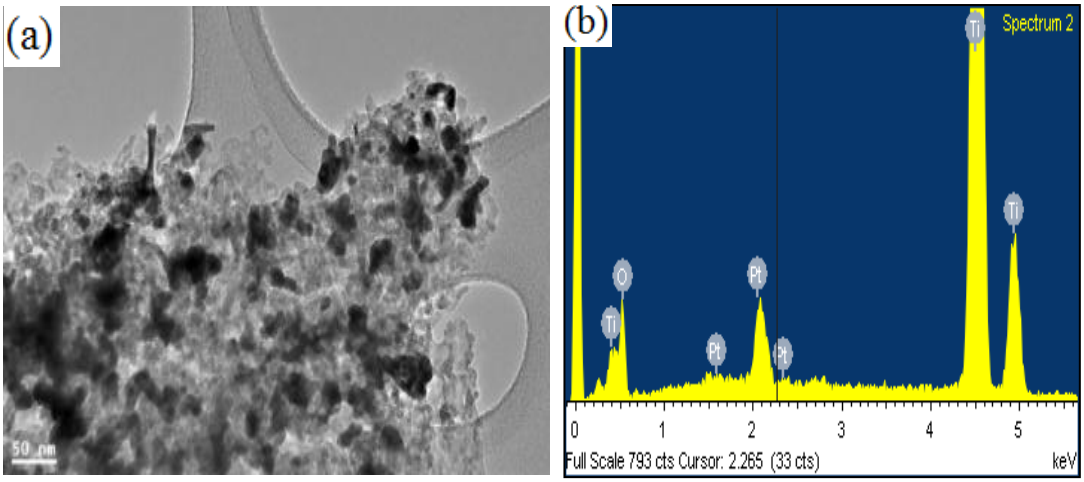

Figure 2. (a) TEM image and (b) EDS for Pt-B/TON-N_2 catalyst.

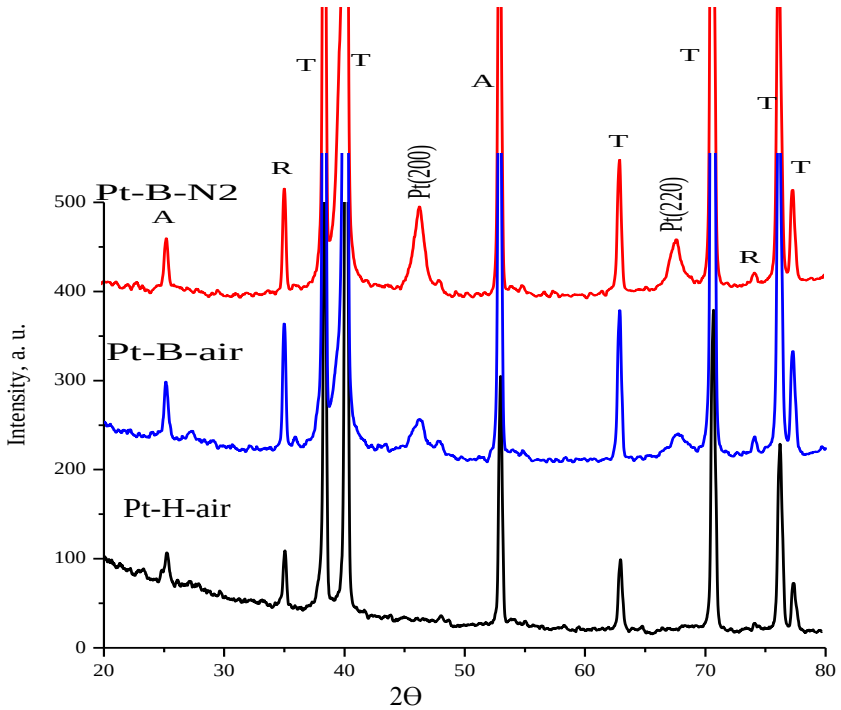

Figure 3. XRD patterns of Pt-H/TON-air (*black*); Pt-B/TON-air (*blue*) and Pt-B/TON-N_2 (*red*).

Figs. 2 shows the TEM images and EDS analysis of Pt deposited on TONs annealed in N_2 at 450 °C for 3 h using $NaBH_4$ (Pt-B/TON-N_2). The EDX graph clearly shows that Pt and Ti are the

major elements of composition which confirm the presence of Pt deposited on TONs substrates. It is difficult to measure the Pt particle size from SEM images but from the TEM image in Fig. 2a we can observe the nanoparticles have large size disruption with a diameter less than 50 nm.Fig. 3 shows the XRD pattern of Pt-H/TON-air, Pt-B/TON-air and Pt-B/TON-N_2 catalysts. The diffraction patterns show the presence of Ti, TiO_2 and Pt phases. The sample Pt-B/TON-N_2 show well defined reflections compared with sample Pt-B-air, indicating a different particle size. From the XRD we can conclude that Pt (200) and Pt (220) crystal faces for Pt-B/TON-N_2 are clearly higher than that for Pt-B/TON-air. This indicates that the degree of preferential orientation of Pt (200) and Pt (220) crystal faces are higher in case Pt-B-N_2 catalysts, which may be attributed to the incorporation of boron with Pt deposit on TONs-N_2, support [41]. On the other hand in case of using hydrazine during preparation of Pt-H-air catalyst, the characteristics diffraction peaks of Pt (200) and Pt (220) mostly can't observe.

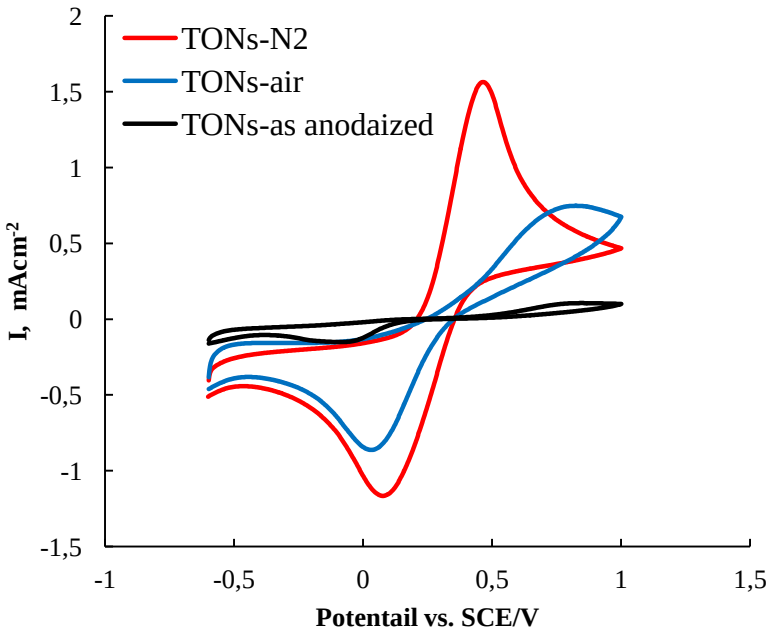

Figure 4. CVs at 50 mVs^{-1} for TON as anodized (*black*); TON-air (*blue*) and TON-N_2 (*red*) in 10 mM $Fe(CN)_6^{3-/4-}$ + 0.1 M KCl solution.

Fig. 4 shows the CVs at 50 mVs^{-1} for TONs-as anodized, TONs-air and TONs-N_2 electrodes in 10 mM $Fe(CN)_6^{3-/4-}$ + 0.1 M KCl. Clearly, the TONs-N_2 electrode shows higher ferri/Ferrocyanide redox peak currents in comparison to the voltammograms obtained for TONs-air and TONs-as anodized electrodes. This can attribute to the greater conductivity and electrochemical active surface area of the TiO_2 nanotubes annealing in N_2 [41].

The electrocatalytic activity of Pt-B/TON-N_2, Pt-B/TON-air and Pt-H/TON-air catalysts towards HER and ORR has been investigated in 0.5 M H_2SO_4 solutions saturated with N_2 or O_2. Fig. 5 shows the cyclic voltammograms at 50 mV s^{-1} for the Pt-H/TON-air, Pt-B/TON-air and Pt-B/TON-N_2 electrodes in N_2 saturated 0.5 M H_2SO_4 solution in potential region from -0.2 to 0.2 V vs. SCE. For the hydrogen adsorption/desorption features, Pt-B/TON-N_2 shows more resolved peaks and higher current

densities than that for Pt-B/TON-air and Pt-H/TON-air catalysts. This can related to the roughness factor for Pt NPs prepared by $NaBH_4$ was higher than that prepared by NH_2NH_2 reducing agent, as shown in table 1. This is partly due to the existence of more Pt (200) and Pt (220) surface sites created by the addition of $NaBH_4$ [42, 43].

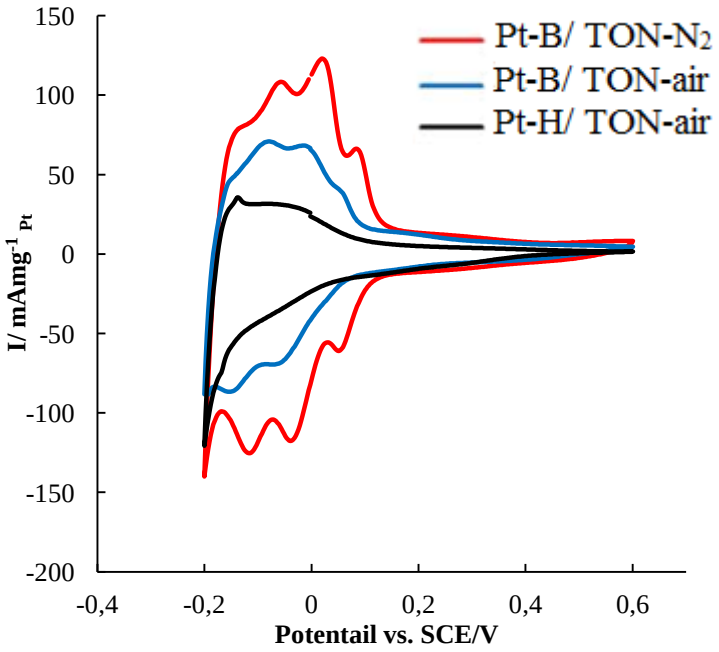

Figure 5. CVs at 50 mVs^{-1} for Pt-H/TON-air (*black*); Pt-B/TON-air (*blue*) and Pt-B/TON-N_2 (*red*) in N_2 saturated 0.5 M H_2SO_4 solution.

Table 1 reports the electrochemical active surface area, roughness factors (R_F) and mass loading of Pt catalysts as measure from hydrogen adsorption/desorption charge and ICP analysis respectively. Within the experimental error, ICP analysis shows that the Pt mass loading for the three catalysts is almost the same. However, the Pt-B/TON-N_2 shows higher roughness factor than that for Pt-B/TON-air and Pt-H/TON-air as shown in Table 1.

Table 1. Electrochemical active surface area and roughness factors (R_F) of Pt NPs on TONs annealed in air and N_2 and deposited by hydrazine and sodium borohydride

Electrode	Q_H m*C*	Surface area (cm^2)	R_F	Mass loading (g cm^{-2})
Pt-H/TON-air	1.05	5.00	7.35	1.32×10^{-5}
Pt-B/TON-air	2.46	11.73	17.25	1.61×10^{-5}
Pt-B/TON-N_2	3.73	17.76	26.11	1.45×10^{-5}

Fig. 6 shows the oxygen reduction CVs at 50 mV s^{-1} for Pt-H/TON-air, Pt-B/TON-air and Pt-B/TON-N_2 catalysts in O_2-satureted 0.5 M H_2SO_4 solution over a potential region from -0.2 to 0.6 V vs. SCE. All the voltammetric profiles show Pt oxide reduction peaks between 0.25 – 0.40 V, which is

the typical potential for oxygen reduction on platinum catalysts in acid solution. Oxygen reduction potential peak is observed at 0.44 V for Pt-B/TON-N_2 while the corresponding value for Pt-B/TON-air and Pt-H/TON-air is observed at 0.38 V and 0.25 V respectively. These results indicate that the Pt-B/TON-N_2 electrode possess higher electrochemical activity for HER and ORR reactions.

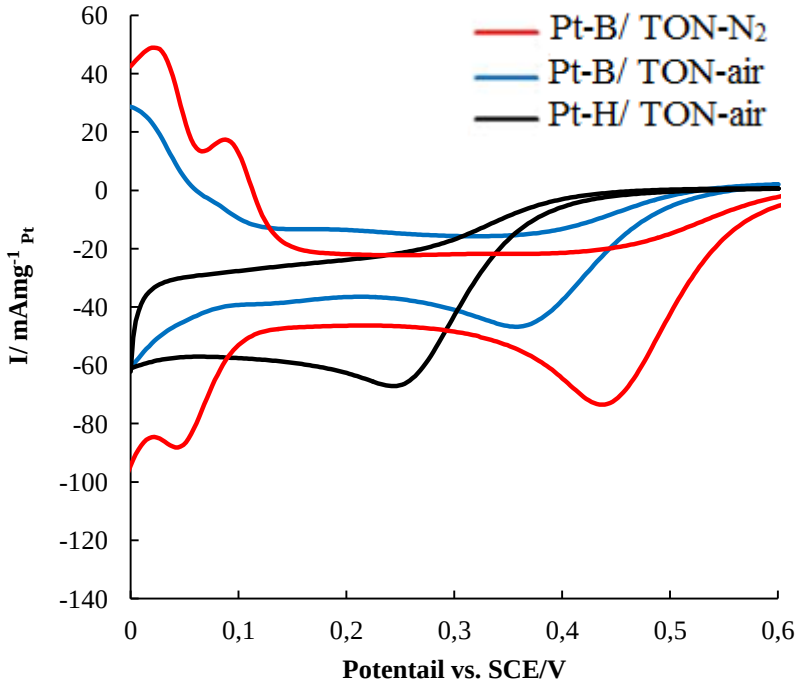

Figure 6. CVs at 50 mVs^{-1} for Pt-H/TON-air (*black*); Pt-B/TON-air (*blue*) and Pt-B/TON-N_2 (*red*) in O_2 saturated 0.5 M H_2SO_4 solution.

The electrocatalytic activity of the catalysts was also investigated for methanol oxidation in acidic and basic media. Fig. 7 shows the CVs for the Pt-H/TON-air, Pt-B/TON-air and Pt-B/TON-N_2 catalysts in 1.0 M methanol and 1.0 M KOH. The peak current densities in the forward scan of the Pt-B/TON-N_2, Pt-B/TON-air and Pt-H/TON-air catalysts are measured to be 540, 380 and 250 $mA{\cdot}mg_{Pt}^{-1}$. It is noted that the peak current is enhanced for catalysts prepared by $NaBH_4$ as reducing agent and TONs annealed in N_2 as a support.

The CV for the Pt-H/TON-air, Pt-B/TON-air and Pt-B/TON-N_2 catalysts in 1.0 M methanol and .5 M H_2SO_4 are shown in Fig. 8 shows. The peak current densities in the forward scan for the Pt-B/TON-N_2, Pt-B/TON-air and Pt-H/TON-air catalysts are 317, 188 and 120 $mA.mg_{Pt}^{-1}$ respectively. The methanol oxidation current density obtained at Pt-B/TON-N_2 catalyst (317 $mA.mg_{Pt}^{-1}$) is higher than that reported for Pt catalyst supported on carbon (159 $mA.mg_{Pt}^{-1}$) [44]. Pt-B/TON-N_2 catalyst shows two times increases in methanol oxidation current in compare with Pt/carbon. Also the Pt-B/TON-N_2 shows the highest peak current density in comparison with Pt-B/TON-air and Pt-H/TON-air catalysts. The ratio of peak currents associated with the anodic peaks in forward (I_f) and backward (I_b) scans is generally used to describe the tolerance of a catalyst to intermediates generated during the oxidation of methanol [45].

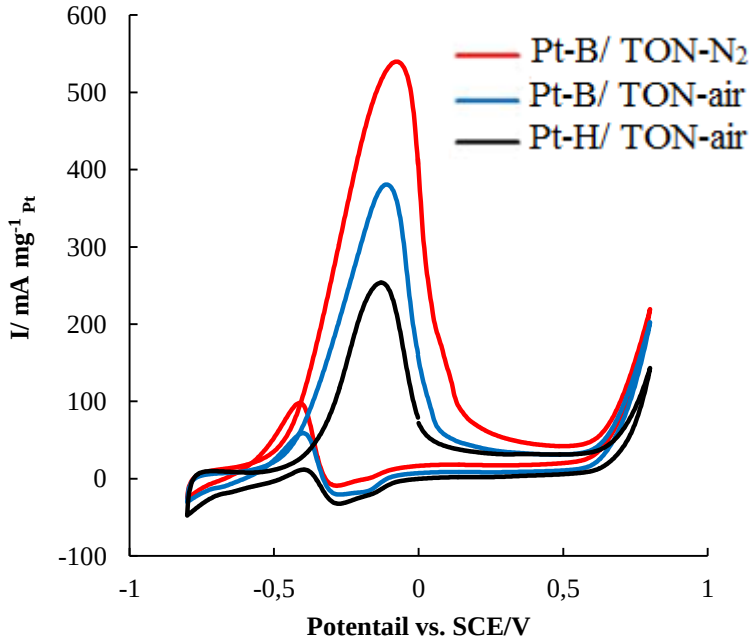

Figure 7. CVs at 50 mVs^{-1} for Pt-H/TON-air (*black*); Pt-B/TON-air (*blue*) and Pt-B/TON-N_2 (*red*) in 0.5 M methanol and 1.0 M KOH solution.

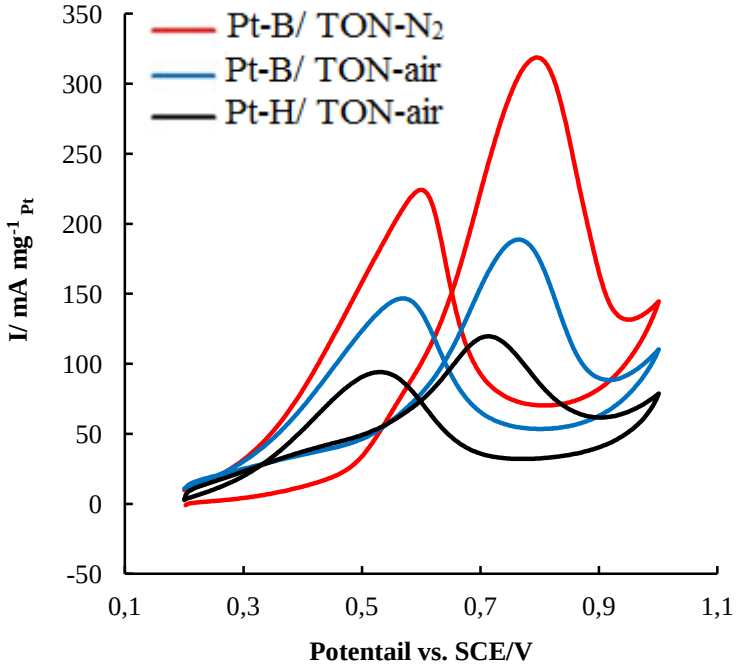

Figure 8. CVs at 50 mVs^{-1} for Pt-H/TON-air (*black*); Pt-B/TON-air (*blue*) and Pt-B/TON-N_2 (*red*) in 0.5 M methanol and 0.5 M H_2SO_4 solution.

A low I_f/I_b ratio indicates poor methanol oxidation to CO_2 during the forward scan, and excessive accumulation of carbonaceous intermediates on the catalyst surface [46]. For our Pt-B/TON-N_2 catalyst, the value of I_f/I_b is 1.42, which is higher than that for Pt-B/TON-air catalyst (1.30), Pt-

H/TON-air (1.26) and about 1.5 times higher than that reported for Pt/carbon (0.95) [44]. The results of the I_f/I_b ratio indicate that the Pt-B/TON-N_2 catalysts exhibits better poison tolerance than that of the others catalyst. The exceptional electrocatalytic performance of the Pt-B/TON-N_2 electrode can be attributed to the synergistic effect of Pt NPs and the TON support on CO oxidation [47], and the ordered structures of TONs can provide unidirectional electronic tubes and reduce the grain boundaries [48]. In addition, the greater conductivity and electrochemical active surface area of the TiO_2 nanotubes annealing in N_2 can contribute to catalytic enhancement [49].

4. CONCLUSIONS

In summary, Pt NPs were chemically deposited on pre-annealed TONs support using hydrazine and sodium borohydride reducing agents. The Pt-B/TON-N_2 electrocatalyst shows a uniform and well dispersion of Pt NPs through the TON with particle size less than 50 nm. The Pt-B/TON-N_2 catalyst has higher electrochemical active area and higher catalytic activity for the oxygen reduction reaction (ORR) and hydrogen evolution reaction (HER) compared with to Pt-B/TON-air and Pt-H/TON-air. Also, the Pt-B/TON-N_2 catalyst exhibits better poison tolerance and two times higher methanol oxidation current density than that reported for Pt/carbon catalyst. This was attributed to the synergistic effect of TON support and Pt NPs and on CO oxidation, the ordered unidirectional structures of TONs tubes and the greater conductivity and electrochemical active surface area of the TiO_2 nanotubes annealed in N_2.

ACKNOWLEDGEMENTS
The authors gratefully acknowledged the financial support by the National Plan for Science and Technology (NPST), King Saud University, Saudi Arabia, Research project; Ref. No.: 08-NAN389-2.

References

1. H. Liu, C. Song, L. Zhang, J. Zhang, H. Wang, D.P. Wilkinson, *J. Power Sources* 155 (2006) 95.
2. B. Mc Nicol, D. Rand, K. Williams, *J. Power Sources* 83 (1999) 15.
3. A. Gamez, D. Richard, P. Gallezot, F. Gloaguen, R. Faure, R. Durand, *Electrochim. Acta* 41 (1996) 307.
4. J. Yu, S. Kang, S. Yoon, G. Chai, *J. Am. Chem. Soc.* 124 (2002) 9382.
5. Y. Shao, J. Liu, Y.Wang, Y.Lin, *J. Mater. Chem.* 19 (2009) 46.
6. N. Shiju, V. Guliants, *Appl. Catal.* A 356 (2009) 1.
7. F. Amano, T. Yasumoto, T. Shibayama, S. Uchida, B. Ohtani, *Appl. Catal. B* 89 (2009) 583.
8. H. Yu, J. Yu, B. Cheng, M. Zhou, *J. Solid State Chem*. 179 (2006) 349.
9. J. Nian, H. Teng, *J. Phys. Chem. B* 110 (2006) 4193.
10. Y. Lan, X. Gao, H. Zhu, Z. Zheng, T. Yan, F. Wu, S. Ringer, D. Song, *Adv. Funct. Mater.* 15 (2005) 1310.
11. J. Nian, H. Teng, *J. Phys. Chem. B* 110 (2006) 4193.
12. Y. Lan, X. Gao, H. Zhu, Z. Zheng, T. Yan, F. Wu, S. Ringer, D. Song, *Adv. Funct. Mater.* 15 (2005) 1310.

13. D. Bavykin, E. Milsom, F. Marken, D. Kim, D. Marsh, D. Riley, F. Walsh, K. El-Abiary, A. Lapkin, *Electrochem. Commun.* 7 (2005) 1050.
14. L. Hou, C. Yuan, Y. Peng, *J. Hazard. Mater.* 139 (2007) 310.
15. D. Bavykin, J. Friedrich, F. Walsh, *Adv. Mater.* 18 (2006) 2807.
16. A. Armstrong, G. Armstrong, J. Canales, P.G. Bruce, *J. Power Sources* 146 (2005) 501.
17. O. Varghese, D. Gong, M. Paulose, K. Ong, C. Grimes, *Sens. Actuators B:Chem.* 93 (2003) 338.
18. J. Macak, H. Tsuchiya, L. Taveira, A. Ghicov, P. Schmuki, *J. Biomed. Mater. Res.* 75A (2005) 928.
19. P. Xiao, B. Garcia, Q. Guo, D. Liu, G. Cao, *Electrochem. Commun*. 9 (2007) 2441.
20. M. Sander, M. Cote, W. Gu, B. Kile, C. Tripp, *Adv. Mater*. 16 (2004) 2052.
21. Q. Chem,W. Zhou, G. Du, L. Peng, *Adv. Mater.* 14 (2002) 1208-1211.
22. J. Macak, H. Tsuchiya, P. Schmuki, Angew. *Chem. Int. Ed.* 44 (2005) 2100.
23. S. Liu, A. Chen, *Langmuir* 21 (2005) 8409.
24. E. Topoglidis, C. Campbell, A. Cass, *J. Durrant, Langmuir* 17 (2001) 7899.
25. R. Vitiello, J. Macak, A. Ghicov, H. Tsuchiya, L. Dick, P. Schmuki, *Electrochem. Commun.* 8 (2006) 544.
26. A. Ghicov, J. Macak, H. Tsuchiya, J. Kunze, V. Haeublein, L. Frey, P. Schmuki, *Nano Lett*. 6 (2006) 1080.
27. V. Tsakova, *J. Solid State Electrochem.* 12 (2008) 1421.
28. A. Esmaeilifar, S. Rowshanzamir, M. Eikani, E. Ghazanfari, *Energy* 35 (2010) 2610.
29. I. Ohno, Mater. *Sci. Eng.* A146 (1991) 33.
30. I. Ron, N. Friedman, D. Cahen, M. Sheves, *Small 4* (2008) 2271.
31. J. Chen, B. Lim, E. Lee,Y. Xia, *Nano Today 4* (2009) 81.
32. E. Antolini, T. Lopes, E. Gonzalez, *J. Alloys Compd.* 461(2008) 253.
33. S. Chu, H. Kawamura, M. Mori, *J. Electrochem. Soc.* 155 (2008) D414.
34. K. Metz, D. Goel, R. Hamers, *J. Phys. Chem.* C 111 (2007) 7260.
35. S. Knupp, W. Li, O. Paschos, T. Murray, J. Snyder, P. Haldar, *Carbon* 46 (2008) 1276.
36. T. Herricks, J. Chen, Y. Xia, *Nano Lett.* 4 (2004) 2367.
37. J. Guo, T. Zhao, J. Prabhuram, C. Wong, *Electrochim. Acta* 50 (2005) 1973.
38. S. Wells, S. Retterer, J. Oran, M. Sepaniak, *ACS Nano* 3 (2009) 3845.
39. MS, AlHoshan AA, BaQais MI, Al-Hazza AM, Al-Mayouf. *Electrochim Acta* 62 (2012) 390.
40. JM. Macak, H. Tsuchiya A. Ghicov, K. Yasuda, R. Hahn, S. Bauer, P. Schmuki, M. Macak, *Mater Sci.* 11 (2007) 3.
41. H. Ma, X. Xue, J. Liao, C. Liu, W. Xing, *Appl. Surf. Sci*. 252 (2006) 8593.
42. Clavilier J, Armand D, *J. Electroanal Chem* 199 (1986) 187.
43. D. Armand, J. Clavilier, *J. Electroanal. Chem.* 233 (1987) 251.
44. X. Zhou, R. Zhang, Z. Zhou, S. Sun, *J of Power Sour* 196 (2011) 5844.
45. Y. NiWu, SJ. Liao, ZX. Liang, LJ. Yang, RF. Wang, *J of Power Sour* 194 (2009) 805.
46. JJ. Wu, HL. Tang, M. Pan, ZH. Wan, WT. Ma, *Electrochim Acta* 54 (2009) 1473.
47. CS. Chen, FM. Pan Appl Catal B-Environ.9 (2009) 663.
48. Q. Zheng, BX. Zhou, J. Bai, LH. Li, ZJ. Jin, *Adv Mater* 20 (2008):1044
49. P Xiao, D. Liu, BB. Garcia, S. Sepehri, Y. Zhang, G. Cao, *Sensors and Actuators B* 134 (2008) 367.